Supplementary Fig.1

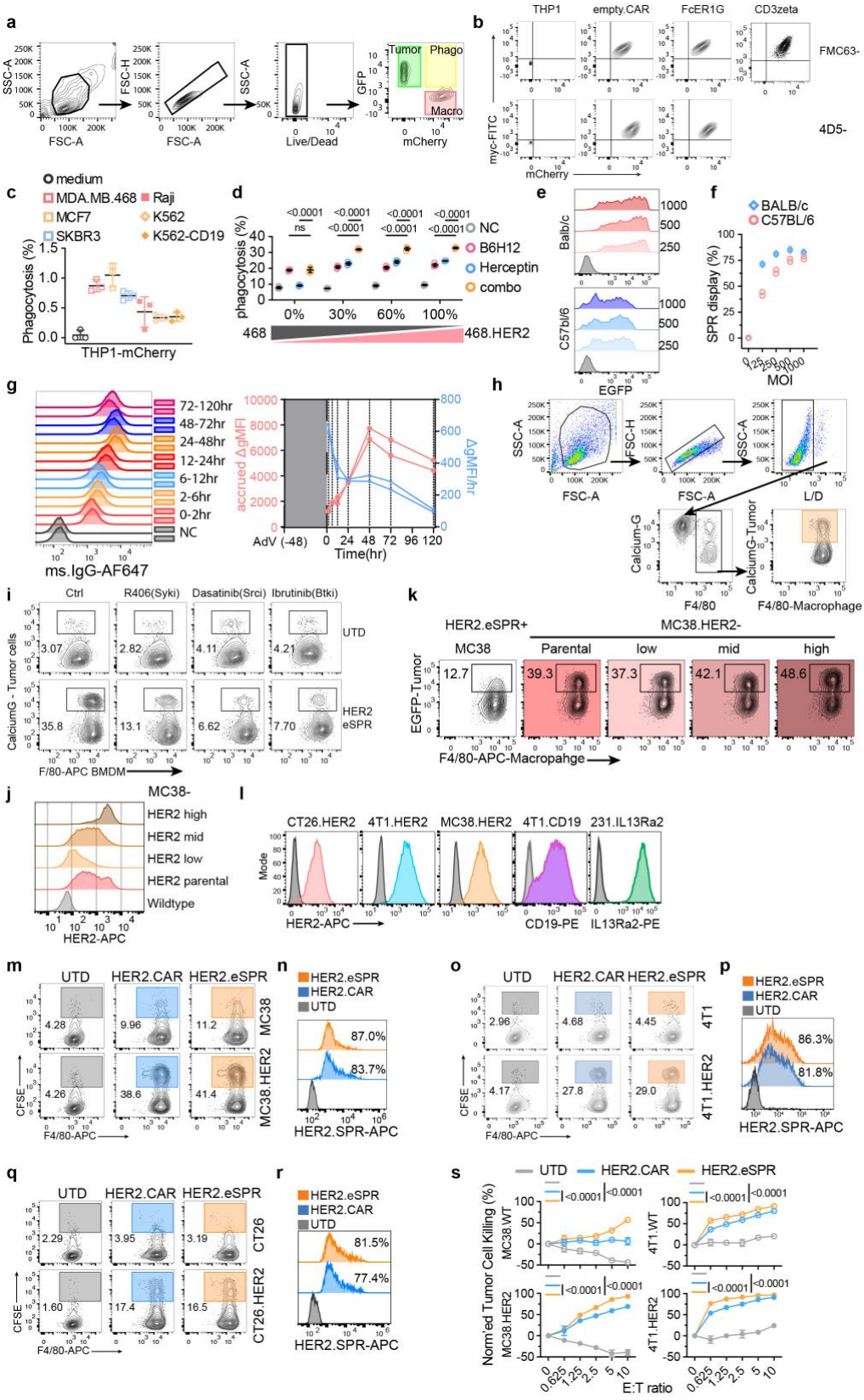

Supplementary Fig.1 *In vitro* validation of the eSPR system in transduced murine macrophages.

a, Gating strategy for PMA stimulated THP-1 cells phagocytosis assay.

b, CARs display purity of sorted CAR-THP1 cells.

c, Basal phagocytosis ratio of THP-1 mCherry cells, without CAR expression.

d, ADCP in synergy with CD47 blockade (n = 4).

e, Ad5 serotype adenovirus penetration to primary murine BMDM cells in vitro.

f, CAR surface display in AdV transduced BMDMs (n=2 for BALB/c, or 3 for C57BL/6).

g, Tumor cell surface staining by the HER2.eSPR macrophages conditioned medium collected in a time-course fashion. CM per 1 macrophage cell was used to stain 10 tumor cells (n=2).

h, Gating strategy for primary murine macrophage flow cytometry assisted phagocytosis assay.

i, Representative flow cytometry scatter plots of the impact of tyrosine kinase inhibitors on CAR-driven macrophage phagocytosis.

j, Representative overlaid flow cytometry histograms of HER2 expression of sorted MC38 target cells stratified by HER2 expression intensity.

k, Representative flow cytometry scatter plots of the HER2 expression intensity on CAR-driven macrophage phagocytosis

l, Representative flow cytometry histograms of antigen expression intensity in stably transduced target tumor cells.

m, Representative flow cytometry scatter plots for flow cytometry phagocytosis assay of macrophages against MC38-derived target cells.

n, HER2.CAR cell surface display intensity of effector macrophages in assay shown in m.

o, Representative flow cytometry scatter plots for flow cytometry phagocytosis assay of macrophages against 4T1-derived target cells.

p, HER2.CAR cell surface display intensity of effector macrophages in assay shown in o.

q, Representative flow cytometry scatter plots for flow cytometry phagocytosis assay of macrophages against CT26-derived target cells.

r, HER2.CAR cell surface display intensity of effector macrophages in assay shown in q

s, Luminescence-assisted tumor cell killing assay of UTD-, HER2.CAR-, or HER2.eSPR-macrophages, at various effector-to-target ratio, incubated with syngeneic MC38 (n=6) or syngeneic 4T1 (n=4) derived target cells for 48 hours.

Bars represent the mean and SD. Statistics were performed using one-way ANOVA with Tukey's multiple comparison test for d; and two-way ANOVA with Tukey's multiple comparison test for s.

Supplementary Fig.2

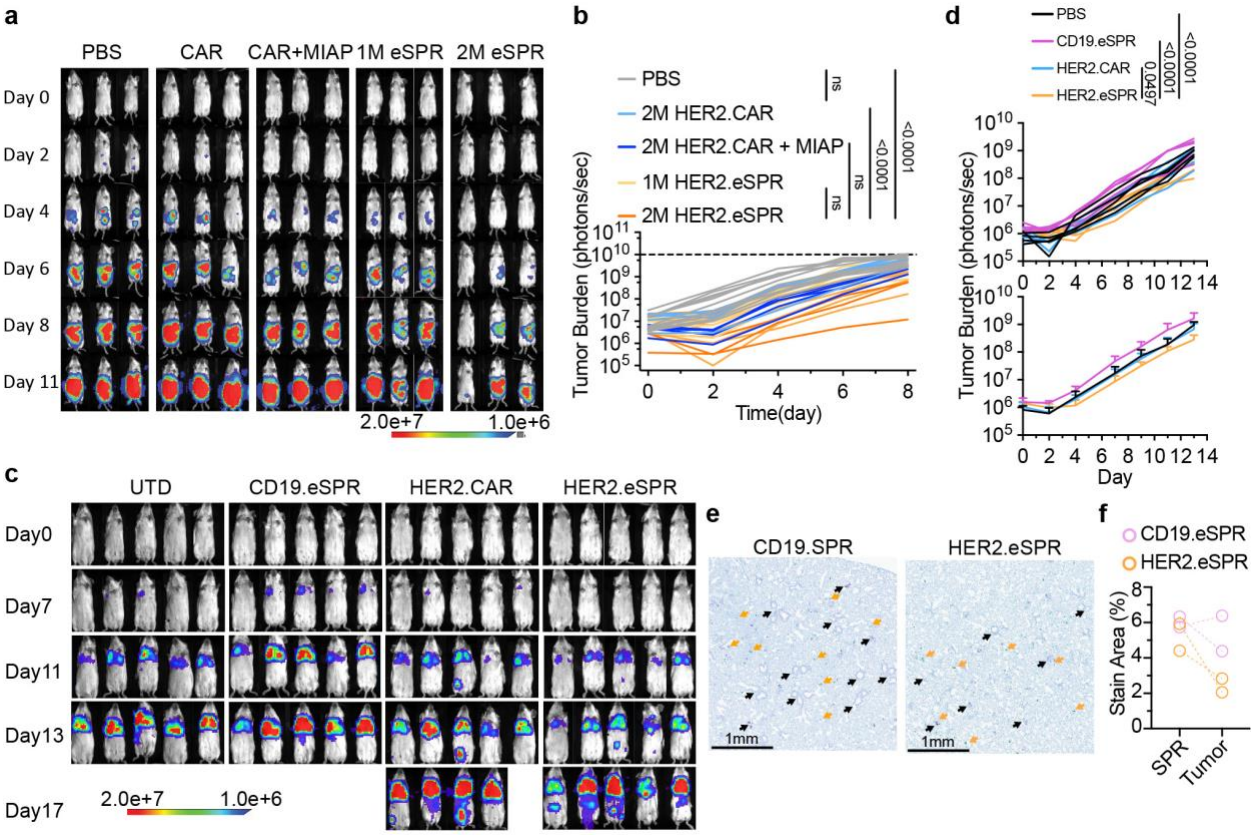

Supplementary Fig.2 HER2.eSPR macrophages conduct direct tumor cell removal *in vivo.*

a, Representative BLI image for carcinomatosis macrophage treatment experiment.

b, Absolute BLI quantified tumor burden for carcinomatosis macrophage treatment experiment.

c, Representative BLI image for lung metastasis macrophage treatment experiment.

d, Absolute BLI quantified tumor burden of individual mouse (top) and group (bottom) for lung metastasis macrophage treatment experiment.

e, Lungs from mice with established metastatic 4T1.HER2 tumor burden treated with transduced macrophages were assessed by duo-color immunohistochemical staining. Black arrows indicated tumor cells, which were stained with anti-HER2 and visualized with purple color; orange arrows indicated transduced macrophages stained with anti-myc.tag (eSPR) and visualized with green color. Each slice represents the lung of one mouse. Bar means 1mm.

f, Quantified relative area intensity for tumor burden and transduced macrophages in the duo-color immunohistochemical stained lungs, using ImageJ software.

Bars represent the mean and SD. Statistics were performed using two-way ANOVA with Tukey's multiple comparison test for b and d.

Supplementary Fig.3

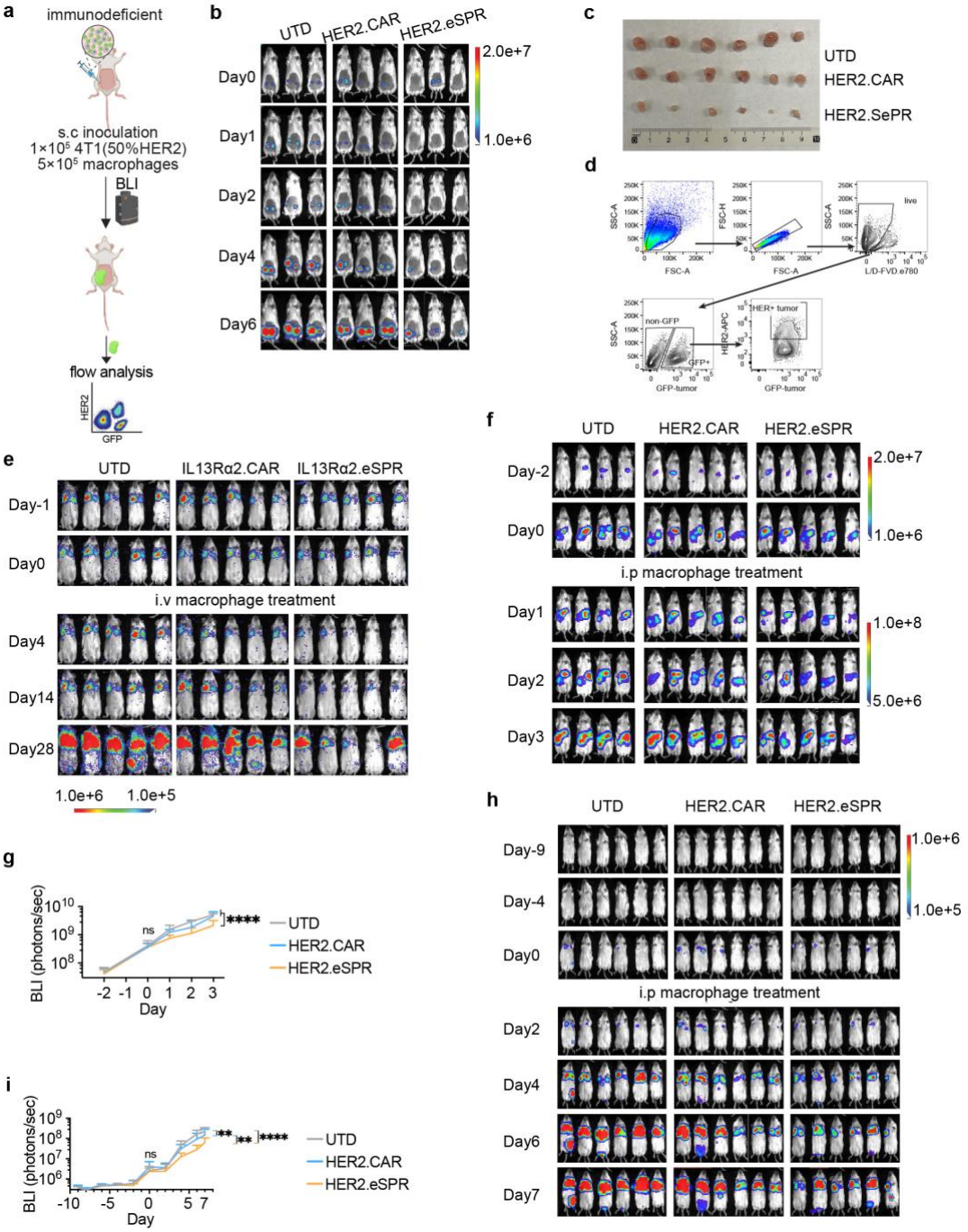

Supplementary Fig.3 eSPR macrophages combat antigen heterogeneous tumor cells in vivo.

a, Schematic overview of the experiment design for macrophage and antigen heterogeneous tumor cells co-inoculation and subsequent flow cytometry assessment.

b, BLI image for macrophage and antigen heterogeneous tumor cells co-inoculation experiment.

c, Tumor tissue extracted on day 12 of the macrophage and antigen heterogeneous tumor cells co-inoculation.
d, Gating strategy and representative scatter plots for flow cytometry tumor tissue HER2 expression analysis.
e, BLI image for IL13Rα2.eSPR macrophage combating antigen heterogeneous established carcinomatosis mouse experiment.
f, BLI image for HER2.eSPR macrophage combating antigen heterogeneous advanced CT26 carcinomatosis immunodeficient mouse experiment.
g, Bioluminescence quantification of advanced CT26 carcinomatosis metastasis burden with one dose of macrophage i.p treatment. Statistical analysis used data on day0 and day3.
h, BLI image for HER2.eSPR macrophage combating antigen heterogeneous advanced CT26 lung metastasis immunodeficient mouse experiment.
i, Bioluminescence quantification of advanced CT26 lung metastasis burden with one dose of macrophage i.v treatment. Statistical analysis used data on day0 and day7.

Statistics were performed using two-way ANOVA with multiple comparison tests for g and i.

Supplementary Fig.4

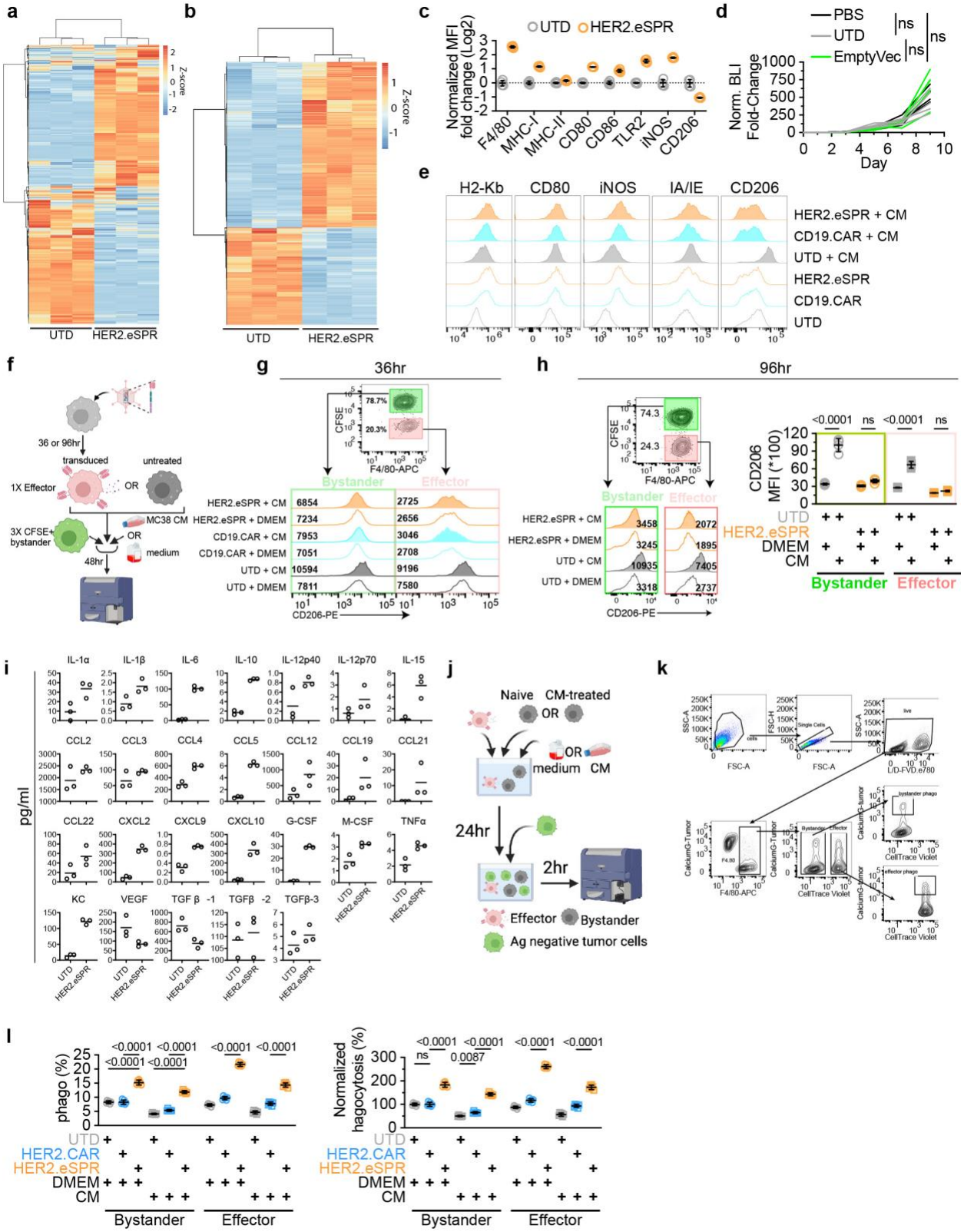

Supplementary Fig.4 Adenoviral transduced eSPR macrophages are phenotypically pro-inflammatory and resistant to tumoral skewing.

a, Hierarchical clustering of differentially expressed genes in NGS bulk RNA sequence from UTD or eSPR transduced murine macrophages (n=3), 48 hours post-transduction.

b, Hierarchical clustering of differentially expressed genes in HPLC-MS/MS proteomics analysis from UTD or eSPR transduced murine macrophages (n=3), 48 hours post-transduction.

c, Normalized MFI quantification of flow cytometry phenotyping of eSPR macrophages, 48 hours post-transduction (n=4), normalized to UTD macrophages.

d, Individual normalized tumor burden growth curve for the 4T1.HER2 carcinomatosis tumor model. BLI was normalized to day 0 baseline of each mouse (n=5).

e, Representative phenotyping flow cytometry histograms of UTD, CD19.CAR, and HER2.eSPR macrophages treated with fresh medium or tumor CM for 48 hours starting 48 hours post-transduction.

f, Schematic cartoon of experiment design for bystander macrophage activation experiment.

g, Representative overlaid histograms for bystander macrophage activation experiment with effector macrophages at 36 hours post-transduction.

h, Representative overlaid histograms and quantified CD206 MFI for bystander macrophage activation experiment with effector macrophages at 96 hours post-transduction.

i, Multiplex secretome quantification of cytokines measured from conditioned medium. Conditioned for 48 hours, starting at 24 hours post-transduction. n=3.

j, Schematic cartoon of experiment design for functional bystander macrophage phagocytic evaluation assays.

k, Flow cytometry gating strategy for the experiment shown in Fig.3J.

l, Phagocytosis ratio and Normalized phagocytosis ratio of bystander and effector macrophages. Normalized to the UTD cells in DMEM for bystander and effector respectively.

Bars represent the mean and SD. Statistics were performed using student's t-test for i; two-way ANOVA with Tukey's multiple comparison test for d and l.

Supplementary Fig.5

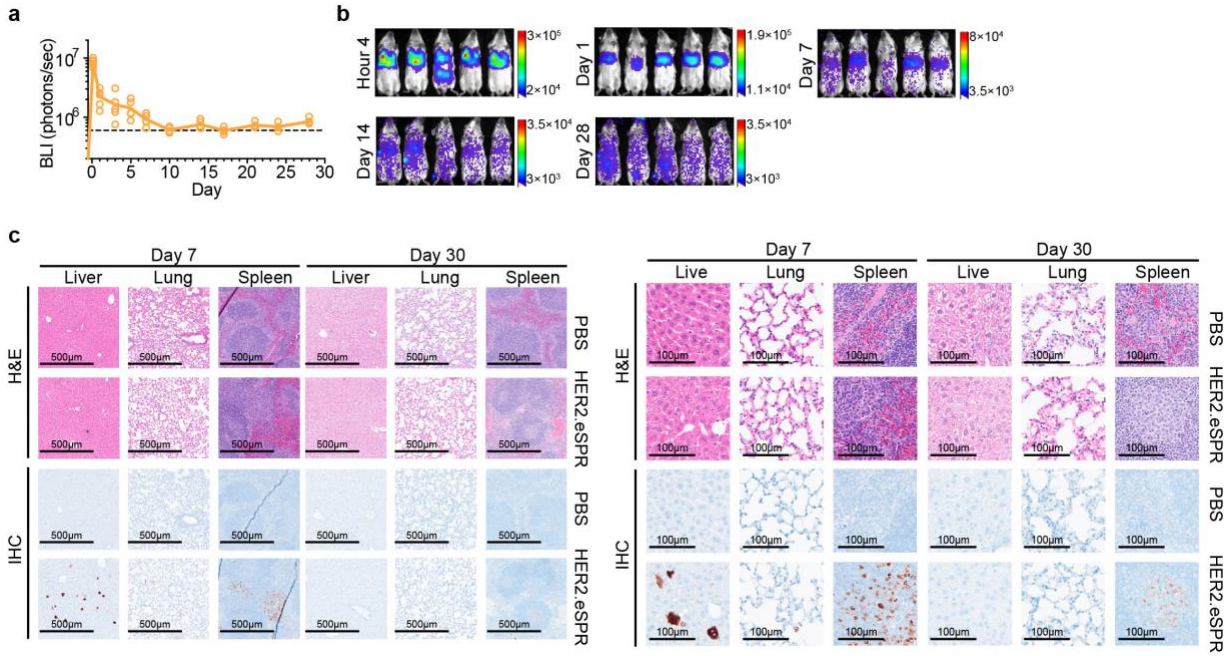

Supplementary Fig.5 HER2.eSPR macrophages showed no detectable somatic tissue damage *in vivo*

a-b, Persistence (a) and biodistribution (b) of HER2.eSPR macrophages in syngeneic immunocompetent BALB/c mice, tracked by in vivo bioluminescence. BMDM cells co-transduced by adenoviral vector carrying HER2.eSPR and firefly luciferase (n=5). The experiment was repeated in C57bl/6 mice with identical conclusions.

c, Histological examination of major organs of B6.HER2 transgenic mice received vehicle or 2 million HER2.eSPR i.v treatment. Organs were collected on day 7 or day 30. Representative view from 2 slides per mouse, 2 mice per condition. Bar means 500 μm and 100μm.

Supplementary Fig.6

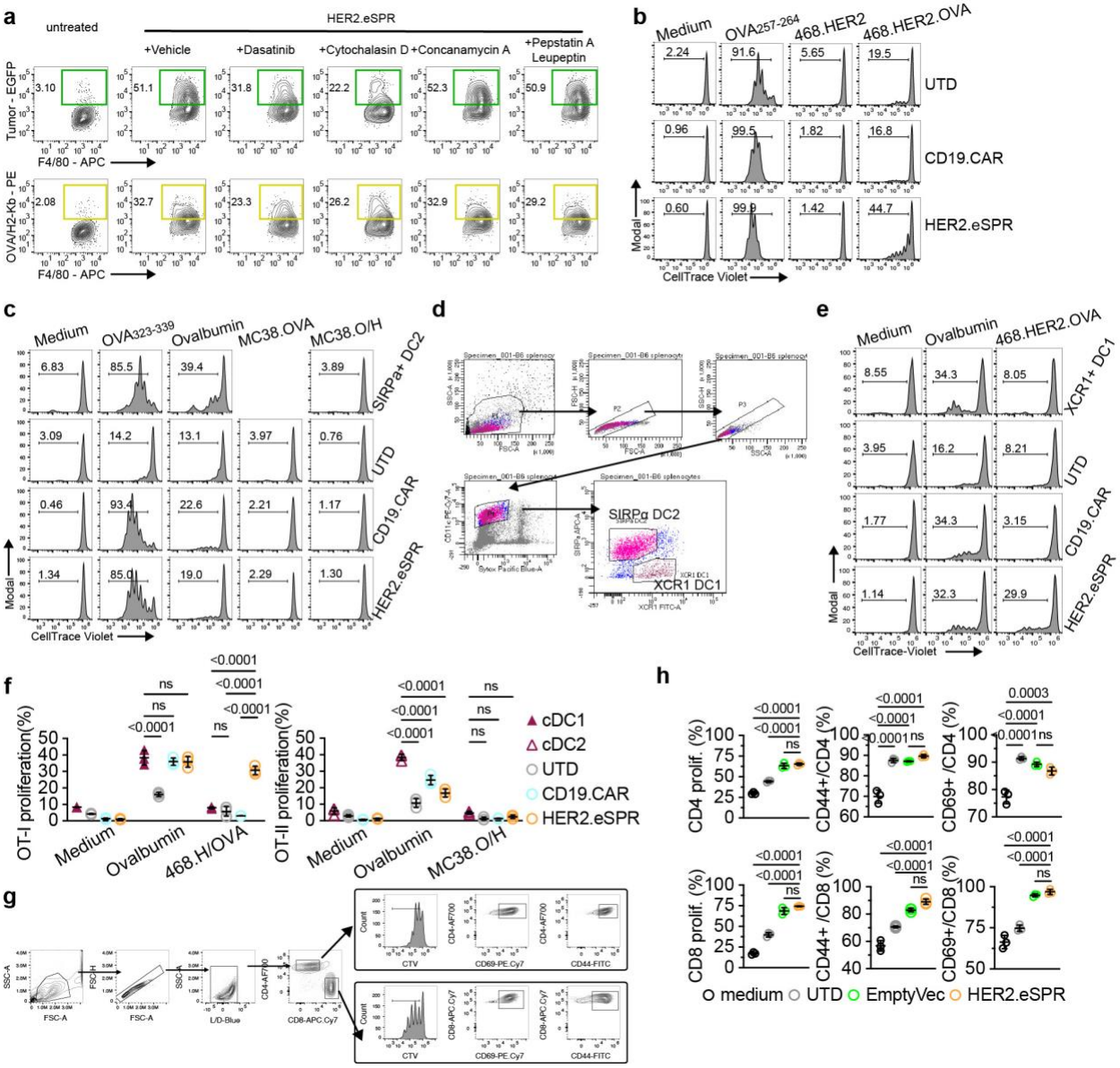

Supplementary Fig.6 eSPR macrophages cross-present antigens derived from phagocytosed tumor cells to activate CD8⁺ T cells.

a, Representative flow cytometry scatter plots of phagocytosis ratio and OVA/H2-Kb display ratio.

b, Representative flow cytometry histograms of OT-I T cell proliferation (Celltrace Violet) in co-culture with macrophages.

c, Representative flow cytometry histograms of OT-II T cell proliferation (Celltrace Violet) in co-culture with macrophages or sorted splenic SIRPα⁺ DC2 cells.

d, Gating strategy for sorting SIRPα$^+$ DC2 and XCR1$^+$ DC1 cells from magnetic beads enriched splenocytes.
e, Representative flow cytometry histograms of OT-I T cell proliferation (Celltrace Violet) in co-culture with macrophages or sorted splenic XCR1$^+$ DC1 cells.
f, Quantification of proliferation or OT-I (left) and OT-II (right) T cells in coculture with macrophages or sorted splenic DCs (n=3).
g, Gating strategy of naïve splenic T cells stimulated by CD3/28 activation beads in the presence of macrophages CM.
h, Proliferation (CTV), CD69 and CD44 expression changes of naïve splenic T cells stimulated by CD3/28 activation beads in the presence of macrophage CM (n=3).

Bars represent the mean and SD. Statistics were performed using two-way ANOVA with Tukey's multiple comparisons for f and h.

Supplementary Fig.7

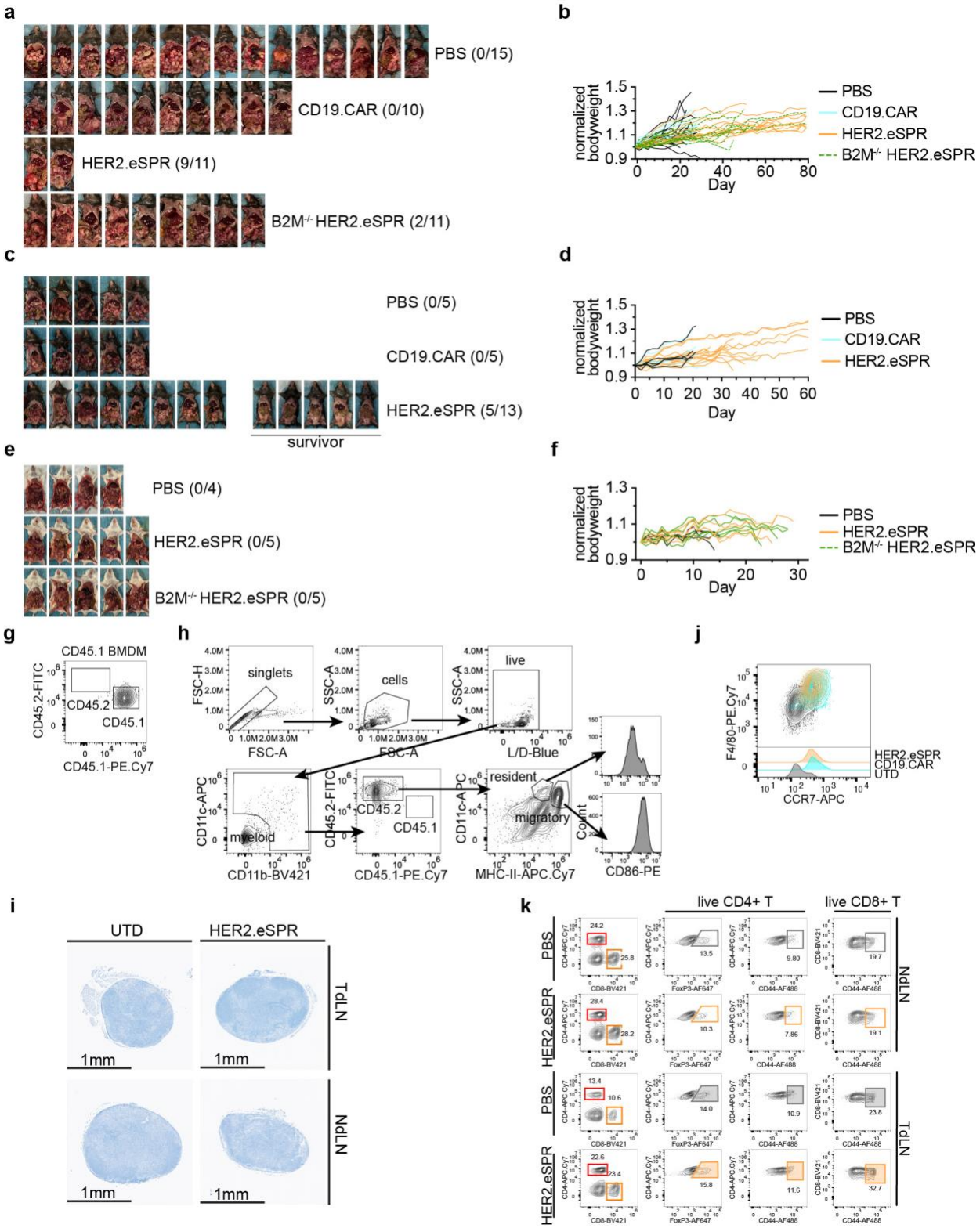

Supplementary Fig.7 eSPR macrophages cross-present to elicit tumor-specific T cell responses without migrating to tumor-draining lymph nodes.

a, Carcinomatosis tumor burden at the humane terminal in the MC38.HER2 carcinomatosis immunocompetent model with early treatment, bracket shows the number of mice that survived the primary carcinomatosis.
b, The normalized body weight curve of mice in MC38.HER2 carcinomatosis immunocompetent model with early treatment.
c, Carcinomatosis tumor burden at the humane terminal in the MC38.HER2 carcinomatosis immunocompetent model with late treatment, bracket shows the number of mice that survived the primary carcinomatosis.
d, The normalized body weight curve of mice in MC38.HER2 carcinomatosis immunocompetent model with late treatment.
e, Carcinomatosis tumor burden at the humane terminal in the MC38.HER2 carcinomatosis immunodeficient model with early treatment, bracket shows the number of mice that survived the primary carcinomatosis.
f, The normalized body weight curve of mice in MC38.HER2 carcinomatosis immunodeficient model with early treatment.
g-h, Positive control (g) of CD45.1 macrophages and gating strategy (h) of lymph node myeloid cells phenotyping.
i, Representative immunohistochemistry staining (myg.tag) of tumor-draining lymph nodes and non-draining lymph nodes extracted on day 3 from MC38.HER2 carcinomatosis-bearing mice received syngeneic macrophages i.p treatment (n=2).
j, Representative flow cytometry of CCR7 expression in control or adenoviral transduced macrophages at day 5 post-transduction.
k, Gating strategy and representative flow cytometry plots of lymphoid cells in tumor-draining lymph nodes and non-draining lymph nodes extracted on day 8 from MC38.HER2 carcinomatosis-bearing mice received syngeneic macrophages i.p treatment.

Supplementary Fig.8

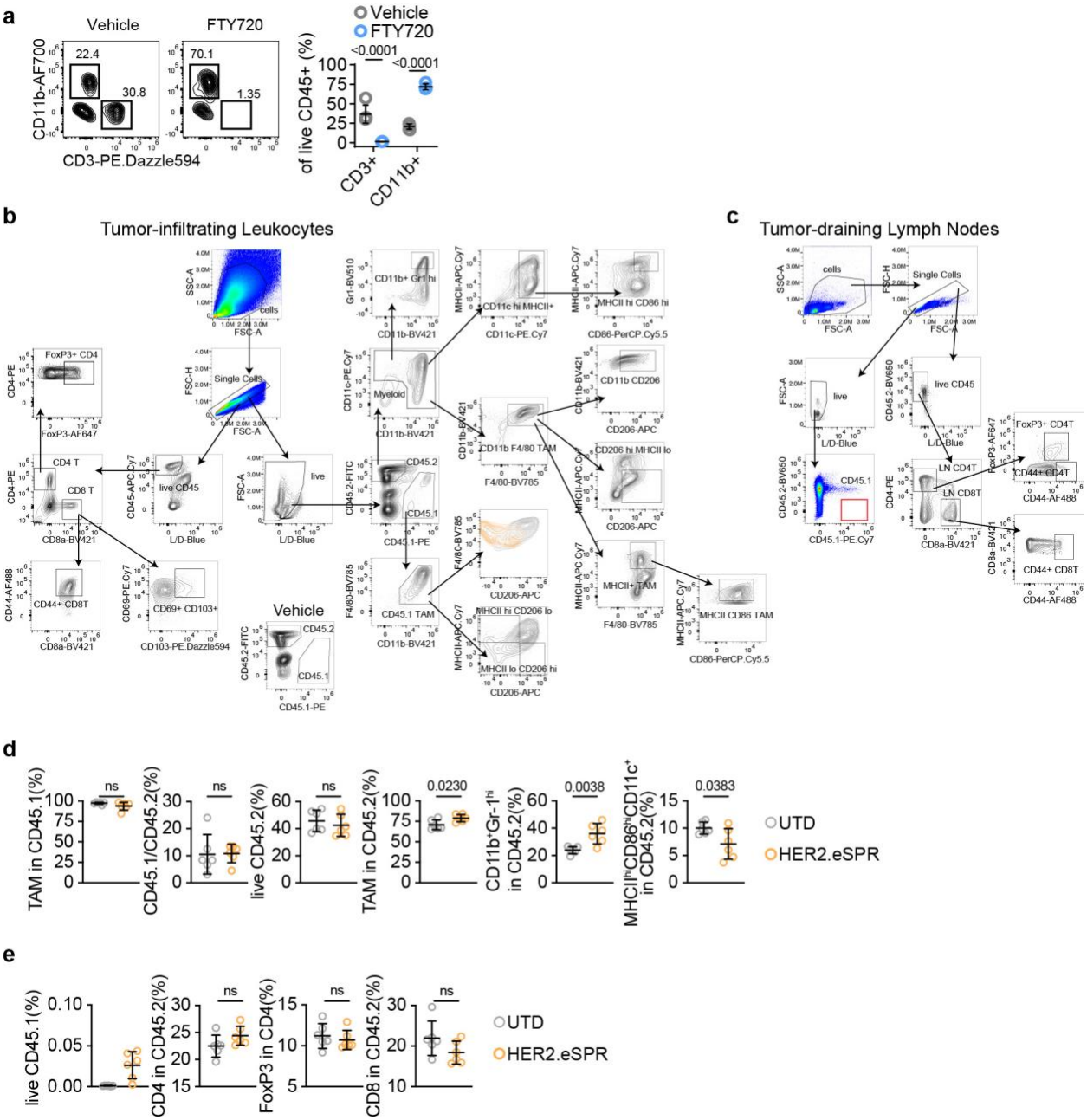

Supplementary Fig.8 HER2.eSPR macrophages elicit inflamed TME.

a, Representative flow cytometry scatter plots (left) and quantification (right) showing the impact of FTY720 on the peripheral circulating T cells.

b, Flow cytometry gating strategy for tumor-infiltrating leukocytes.

c, Flow cytometry gating strategy for tumor-draining lymph nodes.

d, Flow cytometry phenotyping of the tumor-infiltrating leukocytes in MC38.HER2 tumor tissues (n=6).

e, Flow cytometry phenotyping of the tumor-draining lymph nodes in MC38.HER2 subcutaneous tumor model (n=6).

Bars represent the mean and SD. Statistics were performed using one-way ANOVA with Tukey's multiple comparisons for a; two-tailed unpaired student's t-test for d-e.

Supplementary Fig.9

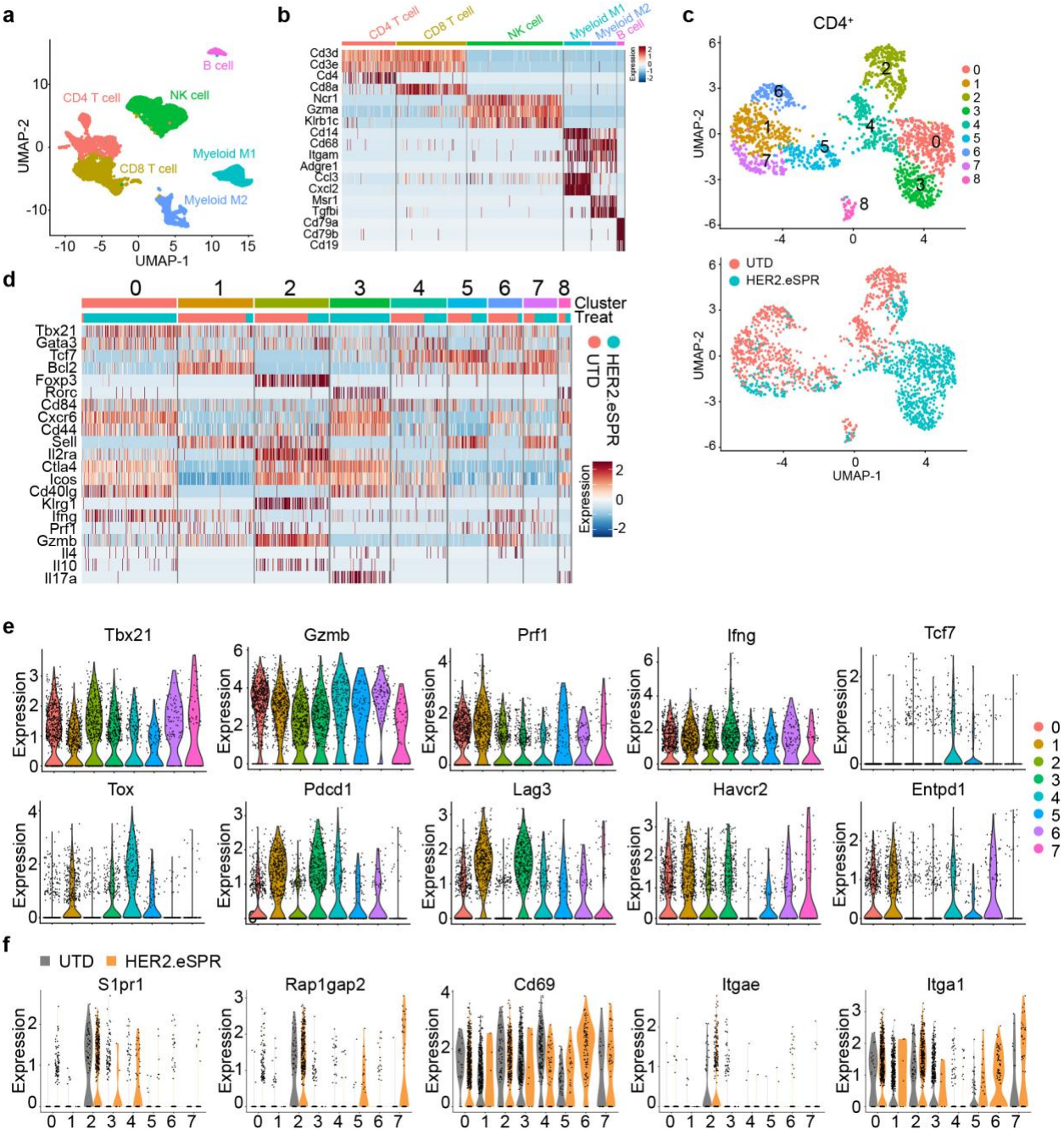

Supplementary Fig.9 HER2.eSPR macrophages immune-edit the TIME.

a, UMAP plot of sorted CD45^{+} tumor-infiltrating leukocytes single-cell RNA-seq clusters in the MC38.HER2 subcutaneous model.

b, Canonical lineage signature gene expression heatmap.

c, UMAP plots showing tumor-infiltrating CD4+ T lymphocyte clusters in the MC38.HER2 subcutaneous model, highlighted by cluster (top) or by treatment (bottom).

d, Representative gene expression heatmap of the CD4+ T cells clusters mirroring clusters in $CD4^+$ UMAP.

e, Selected expression in tumor-infiltrating CD8+ T cells, shown according to clusters.

f, Selected gene expression in tumor-infiltrating $CD8^+$ T cells associated with tissue residency, shown according to clusters, split by treatment.

Supplementary Fig.10

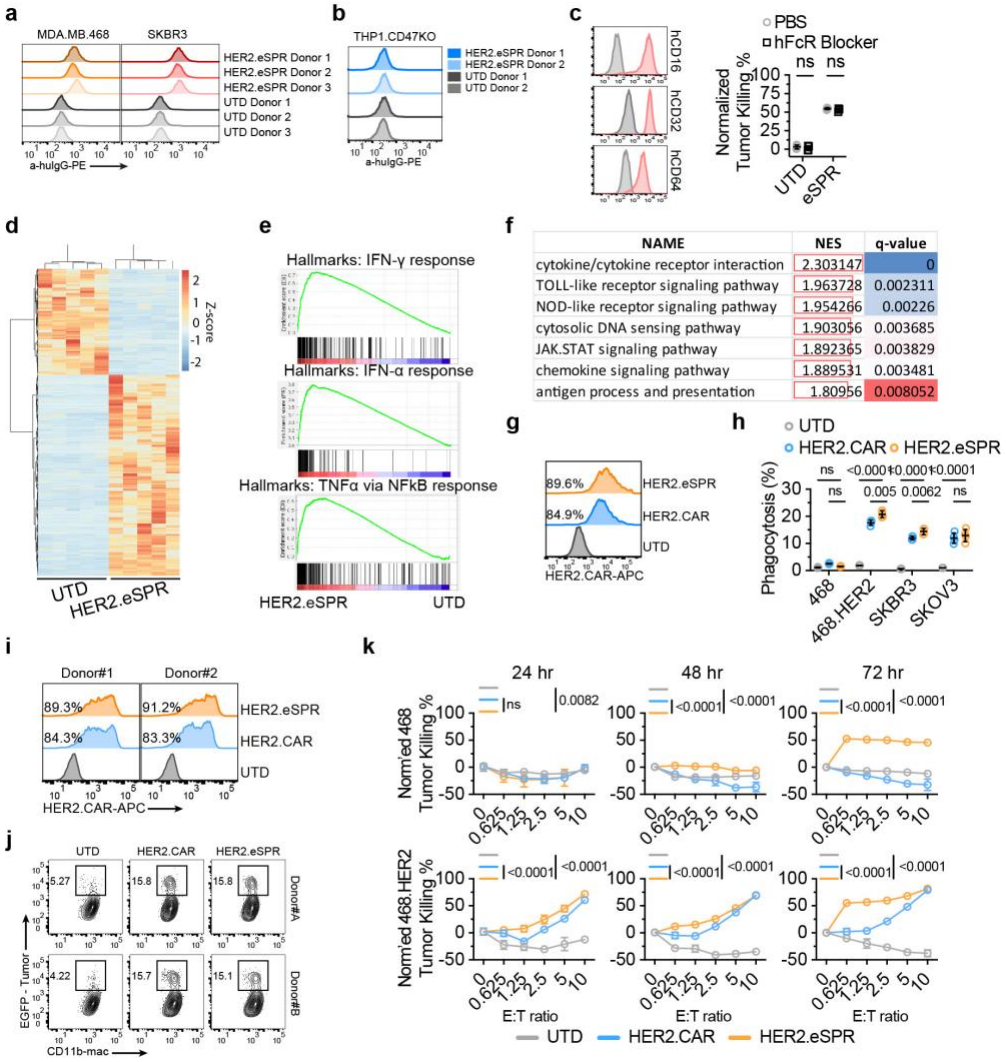

Supplementary Fig.10 Primary human macrophages transduced with the HER2.eSPR.

a, Conditioned medium from HER2.eSPR transduced macrophages functional stain on FcgR-negative MDA.MB.468 and SKBR3 tumor cell lines, indicating binding to tumoral surface CD47 (n=3).

b, Conditioned medium from HER2.eSPR transduced macrophages functional stain on THP1-CD47KO cells (n=2).

c, Luminescence-assisted tumor cell killing assay of B6-hFcR tg macrophages and MDA.MB.468 tumor cells incubated for 48 hours, in the presence of CM from UTD or HER2.eSPR primary human macrophages, conditioned for 48 hours.

d, Hierarchical clustering of differentially expressed genes in NGS bulk RNA sequence from matched UTD or HER2.eSPR transduced human macrophages from 5 healthy donors, 48 hours post transduction.
e, Enrichment plots for the top three enriched pathways in the GSEA, using the human hallmarks molecular signatures database.
f, Top enriched KEGG signal pathways in HER2.eSPR transduced human macrophages.
g, Representative flow cytometry plots for HER2.CAR display on human macrophages.
h, Phagocytosis of UTD, HER2.CAR and HER2.eSPR macrophages in flow cytometry phagocytosis assay with various tumor cells (n=4).
i, HER2.CAR display for human macrophages.
j, Representative flow cytometry phagocytosis scatter plots.
k, Luminescence-assisted tumor cell killing assay of UTD, CAR, or eSPR human macrophages at various effector-to-target ratios, with wildtype or HER2 overexpressed MDA.MB.468 tumor cells (n=4).

Bars represent the mean and SD. Statistics were performed using two-way ANOVA with multiple comparison tests.

Supplementary Fig.11

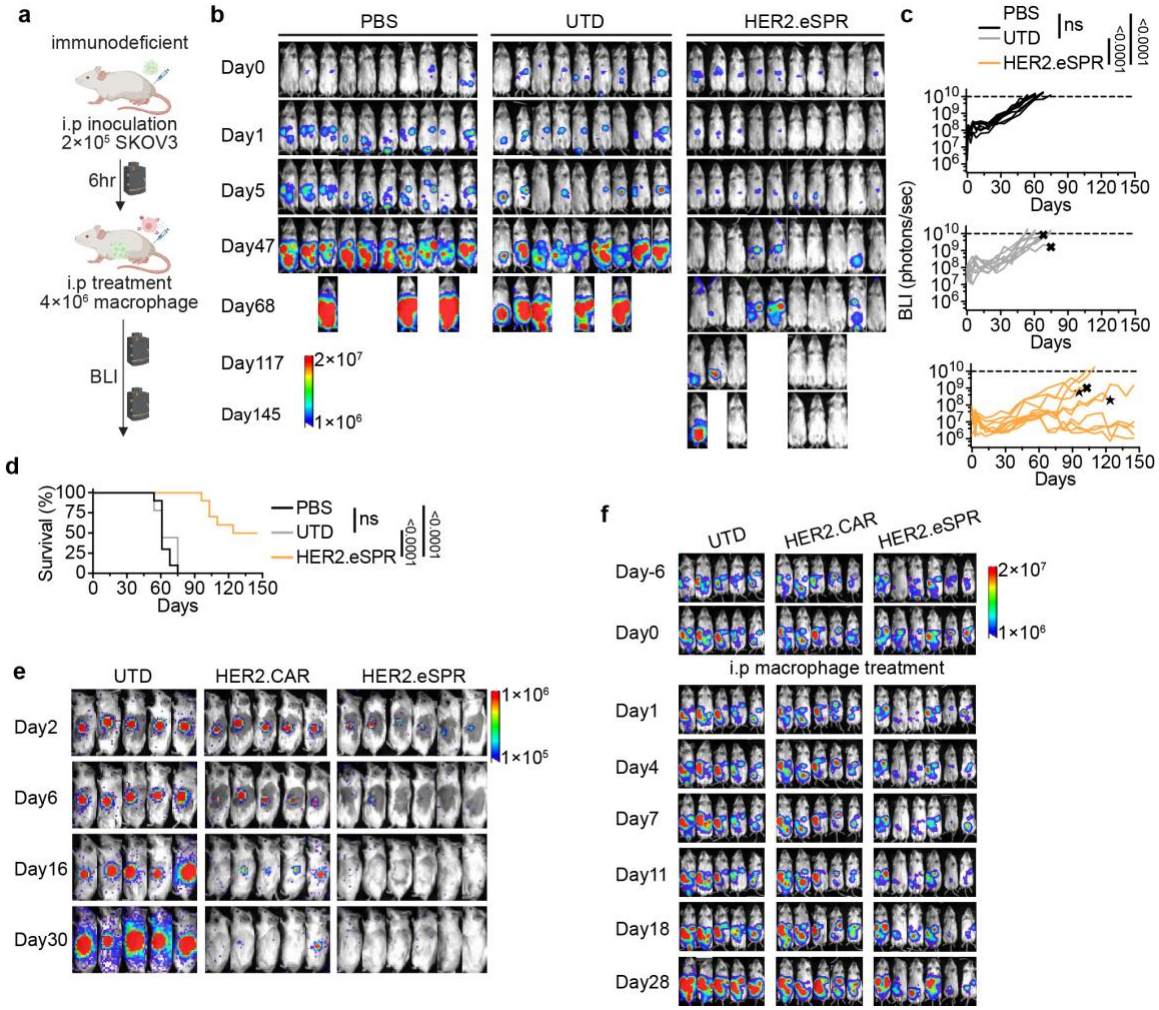

Supplementary Fig.11 HER2.eSPR human macrophages protected human tumor-bearing mice.

a, Schematic overview of the in vivo efficacy experiment for HER2.eSPR human macrophages in early treating SKOV3 carcinomatosis mouse model.

b, BLI image of the HER2.eSPR human macrophages early treatment experiment

c, Individual BLI-measured tumor SKOV3 carcinomatosis burden growth curve with a single dose of macrophage treatment (n=10 for PBS, n=9 for UTD human macrophages, and n=10 for eSPR human macrophages). Data were pooled. Statistical analysis was performed using two-way ANOVA with multiple comparison tests, using data cut-off on experiment day 54. The black cross represents the veterinarian-decided lethargic terminal, asteroid represents the excessive abdominal ascites terminal.

d, Kaplan–Meier survival curve of the HER2.eSPR macrophage early treatment experiment. Statistical analysis was performed using the log-rank Mantel-Cox test.

e, BLI image for the SKOV3 co-inoculation efficacy experiment with human macrophages.
f, BLI image for HER2.eSPR macrophages in efficacy experiment treating established SKOV3 carcinomatosis mouse model.

Bars represent the mean and SD. Statistics were performed using two-way ANOVA with multiple comparison tests.

Supplementary Table.1 Materials and reagents used in this study

Reagent	Source	Identifier
Antibody		
FcR blocking reagent, mouse	Miltenyi Biotec	Cat# 130-092-575
APC anti-human HER2 (24D2)	Biolegend	Cat# 324407
FITC anti-myc (9E10)	Invitrogen	Cat# 13-2511
AF647 donkey anti-mouse IgG	Invitrogen	Cat# A31571
PE goat anti-human IgG Fc	eBioScience	Cat# 12-4998-82
FITC anti-m/h CD11b (M1/70)	BioLegend	Cat# 101206
AF700 anti-m/h CD11b (M1/70)	BioLegend	Cat# 101222
FITC anti-human CD64 (10.1)	BioLegend	Cat# 305005
APC/Fire750 anti-human CD32 (FUN-2)	BioLegend	Cat# 303219
AF700 anti-human CD16 (3G8)	BD Pharmingen	Cat# 557920
BV785 anti-mouse F4/80 (BM8)	BioLegend	Cat# 123141
FITC anti-mouse CD80 (16-10A1)	BioLegend	Cat# 561954
PerCP.Cy5.5 anti-mouse CD86 (GL-1)	BioLegend	Cat# 105028
APC.Cy7 anti-mouse I-A/I-E (M5/114.15.12)	BioLegend	Cat# 107627
Biotin anti-mouse H2Kb (AF6-88.5)	BioLegend	Cat# 116503
APC anti-mouse CD206 (C068C2)	BioLegend	Cat# 141708
PE anti-mouse iNOS (W16030c)	BioLegend	Cat# 696805
BV510 anti-Streptavidin	BD	Cat# 563261
BV785 anti-mouse CD45 (30-F11)	BioLegend	Cat# 103149
APC-Cy7 anti-mouse CD4 (GK1.5)	BioLegend	Cat# 100540
BV421 anti-mouse CD8 (53-6.7)	BioLegend	Cat# 100753
AF488 anti-mouse CD44 (IM7)	BioLegend	Cat# 103016
PE-Cy7 anti-mouse CD69 (H1.2F3)	BioLegend	Cat# 104511
PE.Dazzle594 anti-mouse CD103 (2E7)	BioLegend	Cat# 121429
AF647 anti-mouse FoxP3 (150D)	BioLegend	Cat# 320013
BV421 anti-mouse CD11b (M1/70)	BioLegend	Cat# 101235
PE.Cy7 anti-mouse CD11c (N418)	BioLegend	Cat# 117317
APC anti-mouse F4/80 (BM8)	BioLegend	Cat# 123141
APC.Cy7 anti-mouseI-A/I-E (M5/114.15.2)	BioLegend	Cat# 107627
BV510 anti-mouse Gr-1 (RB6-8C5)	BioLegend	Cat# 108437
PerCP.Cy5.5 anti-mouse CD86 (GL-1)	BioLegend	Cat# 105028
PE anti-mouse CD206 (C068C2)	BioLegend	Cat# 141705
PE anti-mouse CD4 (GK1.5)	BioLegend	Cat# 100413

BV421 anti-mouse CD8 (53-6.7)	BioLegend	Cat# 100753
PE.Cy7 anti-mouse TNFa (MP6-XT22)	BioLegend	Cat# 506323
FITC anti-mouse IFNg (XMG1.2)	BioLegend	Cat# 505805
APC anti-mouse GzmB (QA16A02)	BioLegend	Cat# 372203
APC anti-mouse CD3 (17A2)	BioLegend	Cat# 100235
APC-Cy7 anti-mouse CD4 (GK1.5)	BioLegend	Cat# 100414
APC-Cy7 anti-mouse CD8 (53-6.7)	BioLegend	Cat# 100713
AF700 anti-mouse CD44 (IM7)	BioLegend	Cat# 103025
PE-Cy7 anti-mouse CD69 (H1.2F3)	BioLegend	Cat# 104511
PE anti-mouse OVA/H2kB (25-D1.16)	BioLegend	Cat# 141603
PE.Dazzle594 anti-mouse CD3 (17A2)	BioLegend	Cat# 100245
FITC anti-mouse CD45.2 (104)	BioLegend	Cat# 109805
BV650 anti-mouse CD45.2 (104)	BioLegend	Cat# 109835
PE anti-mouse CD45.1 (A20)	BioLegend	Cat# 110708
PE.Cy7 anti-mouse CD45.1 (A20)	BioLegend	Cat# 110729
APC.Cy7 anti-mouse CD45 (30-F11)	BioLegend	Cat# 103115
APC anti-mouse CD11c (N418)	BioLegend	Cat# 117309
PE anti-mouse CD86 (GL-1)	BioLegend	Cat# 105007
FITC anti-mouse XCR1 (ZET)	BioLegend	Cat# 148209
APC anti-mouse SIRPα (P84)	BioLegend	Cat# 144014
Biotin anti-mouse CD3e (145-2C1)	BioLegend	Cat# 100304
Biotin anti-mouse TER119 (TER-119)	BioLegend	Cat# 116204
Biotin anti-mouse B220 (RA3-6B2)	BioLegend	Cat# 103204
Biotin anti-mouse Gr-1 (RB6-8C5)	BioLegend	Cat# 108404
Biotin anti-mouse Ly6-C (HK1.4)	BioLegend	Cat# 128004

Reagent

human AB serum	Omega Scientific Inc	Cat# HS-20
Fixable Viability Dye e780	eBioscience	Cat# 65-0865-18
CFSE	Invitrogen	Cat# C34554
CellTrace Violet	Invitrogen	Cat# C34557
Live/Dead Fixable Blue	Invitrogen	Cat# L34962
Calcium Green-1 AM	Invitrogen	Cat# C3012
ibrutinib	SelleckChem	Cat# S2680
R406	SelleckChem	Cat# S2194
dasatinib	SelleckChem	Cat# S1031
concanamycin D	Cayman chemical	Cat# 11050
cytochalasin D	Cayman chemical	Cat# 11330
leupeptin	Cayman chemical	Cat# 14026

pepstatin A	SelleckChem	Cat# S7381
Recombinant murine M_CSF	Peprotech	Cat# 315-02
Collagenase I	Gibco	Cat# 17018029
Hyaluronidase	Sigma	Cat# H3506
DNase I	Roche	Cat# 11284932001
Cell Activation Cocktail	BioLegend	Cat# 423301
Brefeldin A	BioLegend	Cat# 420601
BJ5183 Electroporation competent cells	Agilent	Cat# 200154
CD14 MicroBeads, human	Miltenyi Biotec	Cat# 130-050-201
mouse T cell isolation kit	Stemcell Technologies	Cat# 19851
anti-mouse CD47 (MIAP410)	BioXCell	Cat# BE0283
Dynabeads M-280 Streptavidin	ThermoFisher	Cat# 11206D

Mouse

Balb/cJ	The Jackson Laboratory	RRID:IMSR_JAX:000651
C57BL6/J	The Jackson Laboratory	RRID:IMSR_JAX:000664
NOD.Cg-Prkdcscid Il2rgtm1Wjl/SzJ (NSG)	The Jackson Laboratory	RRID:IMSR_JAX:005557
B6.Cg-Pds5bTg(Wap-ERBB2)229Wzw/J (B6-HER2 tg)	The Jackson Laboratory	RRID: IMSR_JAX:010562
C57BL/6-Tg(TcraTcrb)1100Mjb/J (OT-I)	The Jackson Laboratory	RRID:IMSR_JAX:003831
B6.Cg-Tg(TcraTcrb)425Cbn/J (OT-II)	The Jackson Laboratory	RRID:IMSR_JAX:004194
B6.SJL-Ptprca Pepcb/BoyJ (CD45.1)	The Jackson Laboratory	RRID:IMSR_JAX:002014
B6.129P2-B2mtm1Unc/DcrJ (B2m KO)	The Jackson Laboratory	RRID:IMSR_JAX:002087
C57BL6-tg(hFcR)-mFcr(KO) (B6-hFcR tg)	Dr. Jeffrey Ravetch at Rockefeller University	N/A
RAG2$^{-/-}$ γc$^{-/-}$ BALB/c	This study	N/A

Cell lines

THP-1	ATCC	TIB-202
K562	Leo D Wang at City of Hope	N/A
Raji	ATCC	CCL-86
MDA.MB.468	ATCC	HB-132
MDA.MB.231	ATCC	HTB-26
MCF-7	ATCC	CRL-3435
SKBR3	ATCC	HTB-30
SKOV3	ATCC	HTB-77
CT26	ATCC	CRL-2638
4T1	ATCC	CRL-2539
MC38	Defu Zeng at City of Hope	N/A

AD-293	Agilent	Cat# 240085
HEK293T	ATCC	CRl-3216

Recombinant DNA

pShuttle-CMV	Addgene	Cat# 16403
pAdtrack-CMV	Addgene	Cat# 16405
Adeasy-1	Addgene	Cat# 16400
epHIV7	This study	N/A
psPAX2	Addgene	Cat# 12260
pMD2.G	Addgene	Cat# 12259
Her2/ERBB2 cDNA ORF	SinoBiological	Cat# HG10004-M
pCDH-CMV-MCS-EF1-Puro	System Biosciences	Cat# CD510B-1
pCL-neo-cOVA	Addgene	Cat# 25097
pAdtrack-firefly luciferase	This study	N/A
pShuttle-HER2.CAR	This study	N/A
pShuttle-HER2.SPR (murine)	This study	N/A
pShuttle-HER2.SPR (human)	This study	N/A
pShuttle-CD19.CAR	This study	N/A
pShuttle-CD19.SPR	This study	N/A
pShuttle-IL13Rα2.CAR	This study	N/A
pShuttle-IL13Rα2.SPR	This study	N/A